J Neurophysiol 99: 545–553, 2008.
First published November 21, 2007; doi:10.1152/jn.01112.2006.

Maintaining Grip: Anticipatory and Reactive EEG Responses to Load Perturbations

D. Kourtis,* H. F. Kwok,* N. Roach, A. M. Wing, and P. Praamstra
Behavioural Brain Sciences Centre, School of Psychology, University of Birmingham, Edgbaston, Birmingham, United Kingdom

Submitted 19 October 2007; accepted in final form 19 November 2007

Kourtis D, Kwok HF, Roach N, Wing AM, Praamstra P. Maintaining grip: anticipatory and reactive EEG responses to load perturbations. *J Neurophysiol* 99: 545–553, 2008. First published November 21, 2007; doi:10.1152/jn.01112.2006. Previous behavioral work has shown the existence of both anticipatory and reactive grip force responses to predictable load perturbations, but how the brain implements anticipatory control remains unclear. Here we recorded electroencephalographs while participants were subjected to predictable and unpredictable external load perturbations. Participants used precision grip to maintain the position of an object perturbed by load force pulses. The load perturbations were either distributed randomly over an interval 700- to 4,300-ms (unpredictable condition) or they were periodic with interval 2,000 ms (predictable condition). Preparation for the predictable load perturbation was manifested in slow preparatory brain potentials and in electromyographic and force signals recorded concurrently. Preparation modulated the long-latency reflex elicited by load perturbations with a higher amplitude reflex response for unpredictable compared with predictable perturbations. Importantly, this modulation was also reflected in the amplitude of sensorimotor cortex potentials just preceding the long-latency reflex. Together, these results support a transcortical pathway for the long-latency reflex and a central modulation of the reflex grip force response.

INTRODUCTION

Precision grip involves finger and opposed thumb grasping the object on each side (Napier 1956). Grip force, normal to the grasped surfaces, develops friction allowing stabilization of the object against load force tangential to the grasped surfaces. There is ample evidence from behavioral studies for the presence of preparatory increase in grip force in human precision grip. The grip force typically anticipates the load force during self-initiated movements (Flanagan and Wing 1993, 1997; Johansson and Westling 1984) or in response to predictable external load perturbations (Kwok and Wing 2006; Serrien et al. 1999; Turrell et al. 1999; Weeks et al. 2000). Such anticipation is taken as evidence for the involvement of an internal forward model in movement control (Flanagan et al. 2003; Wing and Flanagan 1998). Precision grip tasks that involve resisting a changing external load differ from self-initiated movements and simple lifting tasks due to the presence of a reflex grip force adjustment. The application of a load when holding an object produces a sudden rise in grip force that precedes the voluntary grip adjustment. This reflex response may comprise at least two discernible EMG components. The first one, termed the short-latency reflex, has an onset latency of ~30 ms (for hand muscles) and is of spinal origin (Johansson et al. 1994). The second component is the long-latency reflex with an onset latency of ~60–70 ms. The reflex grip force adjustment is thought to be mediated by cutaneous tactile afferents. Long latency reflexes can also be elicited by angular joint displacements inducing muscle stretch (Lee and Tatton 1975). However, although a transcortical pathway for the reflex is widely accepted for the muscle stretch-mediated long latency reflex, this is uncertain for the cutaneously mediated reflex (Johansson et al. 1994; Macefield et al. 1996b).

There is also uncertainty regarding the cortical basis of predictive grip force control. Human functional imaging studies of anticipatory grip force changes preceding self-initiated movements have found activation in the contralateral primary motor and sensory area, dorsocaudal premotor cortex, caudal supplementary motor cortex, cingulate motor area (Kinoshita et al. 2000) and contralateral parietal operculum, ipsilateral supramarginal gyrus, ipsilateral inferior gyrus pars opercularis (area 44) and contralateral thalamus (Schmitz et al. 2005). Parietal (Ehrsson et al. 2003) and cerebellar (Kawato et al. 2003; Milner et al. 2006) regions have been identified in the coordination of predictive grip with load. Several of these structures have been examined with single-cell recordings in monkeys while they resisted predictable and unpredictable load force perturbations. Although this has yielded evidence for preparatory activity in cerebellar cortex and nucleus interpositus (Dugas and Smith 1992; Monzee and Smith 2004), there is a surprising lack of evidence for preparatory activity in primary motor, lateral premotor, supplementary motor, and cingulate motor areas (Boudreau et al. 2001; Cadoret and Smith 1997; Picard and Smith 1992) to explain preparatory grip force modulation.

The present study used high-density electroencephalographic (EEG) recordings to address the cortical basis of predictive and reactive grip force control in response to load perturbations. Experimental manipulation of the predictability of load force perturbations was expected to influence preparatory slow brain potentials. Furthermore, presence or absence of phasic motor cortical activity at an appropriate latency for the long-latency reflex should be informative regarding the possibility of a transcortical reflex pathway. Finally, an interaction between preparatory and reactive EEG effects in grip force control might shed light on the integration of predictive control and afferent information.

* D. Kourtis and H. F. Kwok contributed equally to this work.

Address for reprint requests and other correspondence: P. Praamstra, Behavioural Brain Sciences Centre, School of Psychology, University of Birmingham, Edgbaston, Birmingham B15 2TT, UK (E-mail: p.praamstra@bham.ac.uk).

The costs of publication of this article were defrayed in part by the payment of page charges. The article must therefore be hereby marked "*advertisement*" in accordance with 18 U.S.C. Section 1734 solely to indicate this fact.

METHODS

Participants

Fourteen participants (8 males and 6 females, aged: 28 ± 8 yr) including the first and last authors participated in the experiment. Twelve were right-handed and none had any history of hand or wrist injuries, psychiatric disorders, or neurological disorders. All the participants provided their informed consent after full explanation of the study.

Task and apparatus

Participants sat comfortably on a chair in a quiet, normally illuminated room with their right forearm and wrist resting on a support and their eyes directed at a fixation cross at 1m distance to reduce eye movements. A manipulandum attached to a lightweight robot (PHANTOM 1.5, Sensable Technologies) was held between the right thumb and index finger (Fig. 1). Two load cells (Nano17, ATI Industrial Automation, Apex, NC), which measured forces and torques in six dimensions, were attached to each side of the object. The signals were sampled at a rate of 500 Hz. There were four blocks of trials, preceded by one practice block. The participants were instructed and supervised during the practice block. The four experimental blocks consisted of two blocks of randomly timed force pulses and two blocks of regularly timed force pulses with the order of the blocks alternating between participants. Each block consisted of 5–10 trial series of 60-s duration. Prior to the start of the experiment, the participants were instructed to hold the object without letting it slip while the manipulandum delivered downward 1 N force pulses of 500-ms duration. For the regular trial series, the interpulse interval was 2 s, and for the random trials, the intervals between pulses were uniformly randomized between 0.7 and 4.3 s. In the random condition, only those force pulses that followed the previous force pulse by ≥2.5 s were used for analysis yielding a total number of trials of 249, compared with 240 for the regular condition. The participants were allowed to rest as long as they wished between blocks to avoid fatigue.

EEG and EMG data acquisition

EEG was recorded continuously with Ag/AgCl electrodes from 128 scalp electrodes. The electrodes were placed according to the 10-5 extension of the International 10–20 electrode system (American Electroencephalographic Society 1994; Oostenveld and Praamstra 2001) using a carefully positioned nylon cap. Vertical eye movements were monitored using two electrooculography (EOG) electrodes positioned under the left and right eye, while horizontal eye movements were monitored using the nearest to the eyes cap electrodes (FFT9h/FFT10h). The ground electrode was placed near the vertex. EMG was recorded from the first dorsal interosseous muscle (FDI) and from the abductor pollicis brevis (APB), using two pairs of Ag/AgCl electrodes.

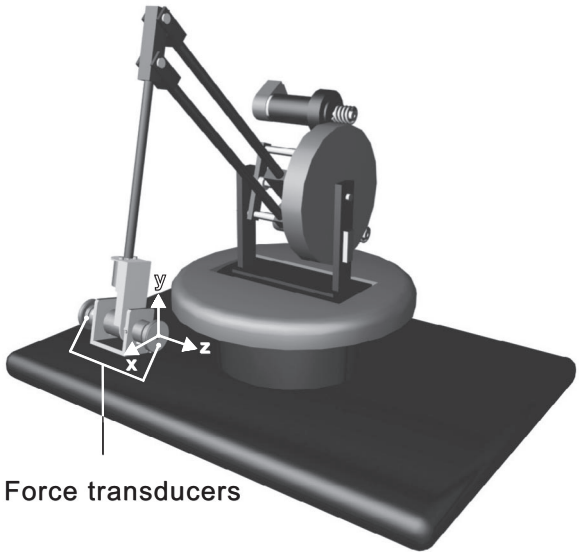

FIG. 1. Diagram of the robotic arm with the manipulandum and the convention for *x, y,* and *z* axes for forces.

The EEG, EOG, and EMG signals were sampled at 1,024 Hz and amplified (DC-256 Hz) by a BioSemi ActiveTwo amplifier (BioSemi, Amsterdam). A trigger was used to send the onset time of the force pulses from the PHANTOM robot to the EEG data acquisition system. Latency measures of EEG and EMG were taken relative to the trigger.

Data analysis

The grip force was derived using the following formula

$$F_G(t) = \frac{|F_{z1}(t)| + |F_{z2}(t)|}{2} \quad (1)$$

where $F_{z1}(t)$ and $F_{z2}(t)$ are the forces along the z axis (Fig. 1) measured by load cell 1 and load cell 2, respectively. The load force was defined as the total measured force orthogonal to the grip force and was given by

$$F_L(t) = \sqrt{F_{x1}^2(t) + F_{y1}^2(t)} + \sqrt{F_{x2}^2(t) + F_{y2}^2(t)} \quad (2)$$

where the subscripts $x1$, $y1$, $x2$, $y2$ refer to the forces in the x and y axis, measured by the two load cells.

The EMG and EEG data were first filtered. The continuous EMG recordings were high-pass filtered at 20 Hz using a fourth-order Butterworth zero phase-shift filter. The EEG was low-pass filtered at 70 Hz using a fourth-order Butterworth zero phase-shift filter. All data (force, EMG, and EEG) were then segmented. Each segment started 1,500 ms before the external load trigger and ended 500 ms afterwards. Artifact processing was performed in the following way. In the case of artifacts in EMG or force signal, the relevant segment was removed for all three measures (force, EMG, EEG). The number of trials thus removed was 1.1 ± 3.4% (mean ± SD) in the regular condition and 0.7 ± 2.7% in the random condition. Because the number of trials affected by an artifact in one (or more) of the EEG channels was far greater (24.5 ± 9.8% for the regular and 23.5 ± 10.5% for the random condition), but equal for both conditions, the corresponding force and EMG signals of those trials were retained. Further details of the analyses of the force, EMG and EEG data are presented in the following text.

Force data

To verify accurate load force timing relative to the load pulses generated by the Phantom robot, a thresholding algorithm was applied to measure load force onset. The section from 500 to 250 ms prior to the trigger of each segment was used as the baseline. A force of 2 SD above the mean baseline load force was used as the threshold. The time when the load force first exceeded this threshold after the trigger was regarded as the onset time. The mean delays were 4.7 ± 0.2 and 5.4 ± 0.2 (SE) ms, respectively, for the regular and random conditions.

For the grip force data, the average force from the first 250 ms of each segment was taken as the baseline and subtracted from the force data. The baseline-corrected segments were then averaged separately for each participant and condition. Preparatory force adjustment was assessed on the basis of the mean amplitude from −500 to 0 ms before the load perturbation. A paired *t*-test was used to compare the response in the two conditions. For comparison of the grip force responses after the load perturbation, the grip force was re-baselined to the mean amplitude in the 100 ms before the load force onset.

EMG data

The continuous EMG recordings were rectified and checked for artifacts due to electrode movement in a semi-automatic artifact rejection procedure. For the analysis of EMG preparatory activity, the baseline was defined as the mean amplitude in the window from 1,000 to 800 ms before load onset, whereas for the long-latency reflex, the baseline adopted was from 100 to 0 ms before load onset. The onset latency and peak latency of the long-latency reflex were detected automatically within selected time windows, and checked visually. The amplitude was measured at peak latency.

EEG data

EEG data processing used BrainVision Analyser software (Brain-Products GmbH, Gilching, Germany). Artifact rejection was performed semi-automatically on the basis of artifact thresholds determined individually. For each participant, the segments from each condition (random or regular) were then averaged and baseline corrected. For analysis of the preload activity, the baseline was defined as the period from 1,400 to 1,200 ms before load onset, whereas for the postload activity, the baseline was defined as the period from 200 to 0 ms before load onset. All EEG signals were analyzed with respect to the common average reference.

EEG preparatory activity was analyzed by pooling the slow brain potential amplitude values of a set of neighboring electrodes over the midline central scalp area, identified on the basis of the scalp distribution of the grand average data. Phasic sensorimotor cortex activity immediately preceding the long-latency reflex was analyzed on the basis of a composite amplitude measure. This measure was computed as the sum of the (absolute) amplitude values taken at the negative and positive polarity maxima of this activity's dipolar field distribution, i.e., electrodes F1 and CP3, respectively. The same activity was also analyzed by means of a dipole source analysis (see following text). Differences between the regular and the random condition were evaluated by means of paired *t*-test.

Dipole source analysis

Dipole source analysis was performed using Brain Electrical Source Analysis software (BESA 5.1.2, MEGIS software GmbH, Gräfelfing, Germany). The analysis was applied to quantify the sensorimotor cortex activity immediately preceding the long-latency reflex. This activity was represented in a phasic component peaking at 58 ms, designated as N58-P58 by analogy to the N54-P54 identified by MacKinnon et al. (2000) as a cortical contribution to the generation of the long latency reflex. The advantage of quantifying this component in terms of dipole strength is that this approach takes the entire scalp distribution into account. The analysis used the standard BESA volume conductor head model, i.e., a four-shell ellipsoidal head model (head radius: 85 mm; brain conductivity: 0.33 mho/m; scalp thickness: 7 mm and conductivity :0.33 mho/m; bone thickness: 7 mm and conductivity: 0.0042 mho/m; cerebrospinal fluid thickness: 1 mm and conductivity: 1 mho/m). The N58-P58 component was modeled for each participant by one regional source, which was subsequently reduced to a single dipole source. No constraints were imposed on the dipole in terms of location or orientation. Dipole source coordinates were specified in Talairach-Tournoux coordinates, and the orientation in theta and phi angles, which correspond to the azimuth and the polar angle, respectively.

The strategy of modeling the isolated N58-P58 component as opposed to a spatiotemporal modeling procedure for the entire epoch (cf. MacKinnon et al. 2000) was chosen because this approach is less susceptible to bias by subjective decisions on modeling parameters. The potential drawback of not accounting for overlapping activity from other sources was deemed less relevant, since single dipole models explained the data with reasonable goodness of fit. This was not the case, however, in three participants (*4, 7,* and *12*) in whom the N58-P58 in the regular condition could not be adequately modeled with a single dipole due to temporal preparation effects in the form of enhanced alpha/mu activity over the right hemisphere. A principled approach of modeling this activity on the basis of narrow (8–12 Hz) band-pass filtered data, with a single dipole, was only successful in two out of the three participants. As a simple alternative approach, applicable in each of the three participants, the activity was modeled by fitting an additional single dipole simultaneously with the N58-P58 dipole. This dipole assumed a location in parietal/sensorimotor cortex of the right hemisphere. For comparisons between regular and random condition, this dipole was also added to the model for the random condition in these three participants.

The dipole solutions for each participant were assessed by three criteria: the residual variance (RV) as a measure of how well a dipole source model explains the recorded data, the dipole source location and orientation should be in agreement with the scalp topography, and the solution should be neurophysiologically plausible. The dipole onset and peak latencies, along with the dipole moment magnitudes were quantified for both the regular and the random condition and compared using a paired *t*-test.

RESULTS

Force data

The mean baseline grip force was 6.5 ± 1.6 and 6.4 ± 1.6 (SE) N for the regular and random conditions, respectively. The difference was not statistically significant. The grand average grip force response to the random and regular load force perturbations are shown in Fig. 2 along with the EMG and EEG responses. In the random condition, the preload grip force did not vary significantly from the baseline, and the grip force increased only after the trigger. In contrast, in the regular condition, there was a slow rise in the grip force preceding the trigger, and the grip force rose further after the trigger. The average grip force in the 500-ms interval before the load force onset was higher in the regular condition compared with the random condition [0.089 ± 0.027 vs. 0.030 ± 0.012 N; $t(13) = -3.39$, $P = 0.0049$].

To analyze the grip force response after the load perturbations, the signals were re-baselined to the mean amplitude in the 100 ms before the load force onset. Thus aligned, the grip force response in the random condition was higher than in the regular condition with waveforms separating around the latency of 100 ms. The amplitudes were compared in 25 ms overlapping 50-ms time windows from 100 to 300 ms. Results showed that the difference between the random and regular condition started to become statistically significant at 150 ms. In the time window between 175 and 225 ms (around the grip force peak), the baseline-corrected grip force was 0.56 ± 0.04 and 0.68 ± 0.06 N [$t(13) = 2.80$, $P = 0.015$), respectively, in the regular and random condition.

In both conditions, the rise in the grip force after the trigger coincided with the load force change and preceded the EMG response. We believe that this was due to mechanical factors. We conducted a test by replacing the human fingers in the experimental setting with a pair of rubber pads and delivered a downward load force using the PHANTOM. This resulted in an immediate increase in the measured *z*-axis force, directly corresponding to the change in load force applied to the *x* and *y* axes. This could be due to mechanical interaction between the 6 dof transducers and fingerpads or due to the support

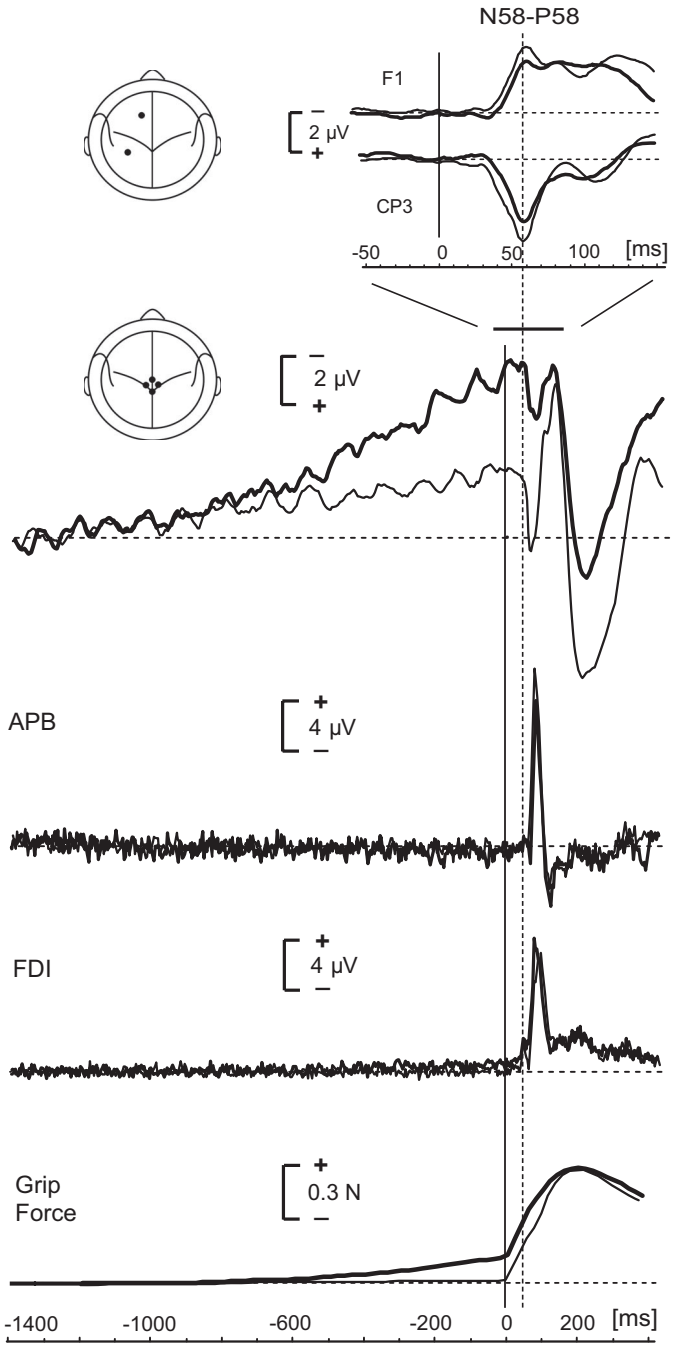

FIG. 2. Grand average of (from top to bottom) the N58-P58 sensorimotor cortex activity, preparatory slow brain potentials at central midline electrodes (Cz, CPz, CCP1h, and CCP2h), electromyographic (EMG) activity from m. abductor pollicis brevis (APB) and m. interosseous dorsalis I (FDI), and grip force recording. The horizontal dashed lines represent the baseline. Thin lines refer to the random condition and bold lines to the regular condition. The solid and the dashed vertical lines represent load onset and N58-P58 peak latency (i.e., 58-ms post load onset), respectively.

structure of the transducers. The early grip force rise does not affect the evaluation of EEG and EMG data.

EMG analysis

As shown in the grand average EMG data (Fig. 3), there was a small difference in the preload activity in the FDI muscle between random and regular conditions with an anticipatory increase of EMG activity for the regular condition, which started ~500 ms and became more evident ~300 ms before load onset. By contrast, no such modulation was found for the APB. Consequently, the analysis regarding the preparatory EMG activity was restricted to the FDI muscle. The mean amplitude from 500 to 0 ms before load onset was higher in the regular condition; the difference was assessed by means of a paired *t*-test and it was found to be statistically significant [$t(13) = -3.273$, $P = 0.006$].

The post load onset EMG waveforms revealed an EMG component in both muscles, the latency of which was too long to be a spinal reflex and too short to be a voluntary response. Specifically, for the ABP muscle the onset latency was 63.5 ± 0.9 and 63.7 ± 0.7 (SE) ms for the regular and random conditions, respectively, whereas the peak latency was 84.8 ± 1.3 and 85.5 ± 1.9 ms for the regular and random conditions, respectively. The amplitude was 12.0 ± 3.1 and 16.0 ± 4.5 μV for the regular and random conditions, respectively. For the FDI muscle, the onset latency was 63.9 ± 1.4 and 63.7 ± 1.1 ms for the regular and random conditions, respectively, whereas the peak latency was 86.7 ± 2.1 and 89.1 ± 2.4 ms, respectively. The amplitude was 10.5 ± 4.4 and 9.9 ± 2.7 μV for the regular and the random conditions, respectively. This response presumably reflects the long-latency reflex (LLR), the generation of which may involve a transcortical loop.

The magnitude of the LLR, recorded from the APB muscle, was higher in the random condition. This difference was evident in the grand average data (Fig. 4), and, by means of a paired *t*-test, it was found to be statistically significant [$t(13) = 2.194$, $P = 0.047$]. The magnitude of the LLR recorded from the FDI muscle was higher in the random condition for 11 of 14 participants. However, this result was not reflected in the grand average data (Fig. 4), mostly due to *participant 9,* who showed an exceptionally high response, which was higher in

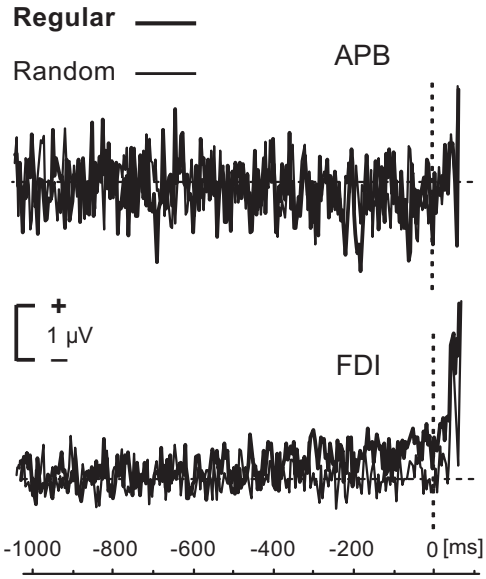

FIG. 3. Grand average EMG traces from 1,000 ms before the load onset to 50 ms after the load onset recorded over the APB and the FDI muscles. The vertical axis (*time 0*) represents load onset. The horizontal dashed line represents baseline. There is an increase in EMG activity, recorded over the FDI muscle, in the regular condition (thick line) starting around 500 ms before load onset.

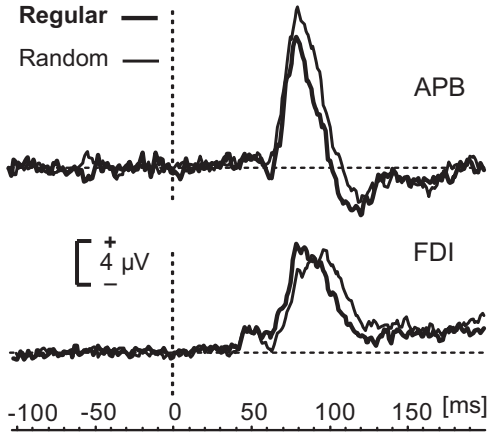

FIG. 4. Grand average EMG traces recorded over the APB and the FDI muscles showing the long latency reflex (LLR) for both the random (thin line) and the regular condition (thick line). The vertical axis (*time 0*) represents load onset. The horizontal dashed line represents baseline.

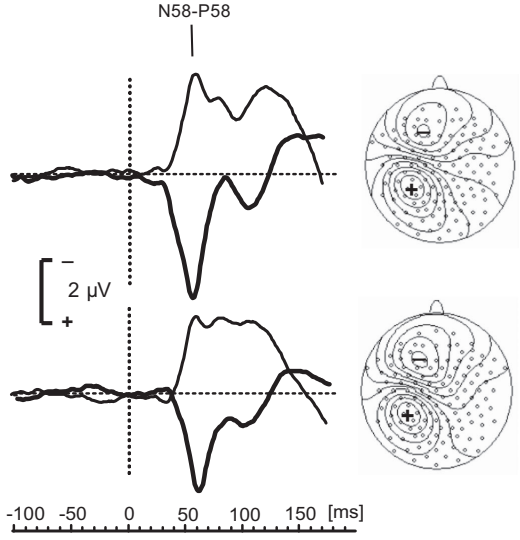

FIG. 6. The N58-P58 component as represented in waveforms recorded from electrodes F1 (thick line) and CP3 (thin line) and in scalp topographies for the random (*top*) and the regular condition (*bottom*).

the regular condition. Therefore the FDI LLR magnitude was assessed by means of a nonparametric sign test. This analysis showed a higher LLR magnitude in the random over the regular condition that nearly reached significance ($P = 0.057$; 2-tailed). Nonparametric evaluation of the LLR recorded from the APB yielded the same values ($P = 0.057$; 2-tailed).

We also examined whether the modulation of the LLR magnitude was influenced by the amplitude of the background EMG activity. Nonbaseline corrected EMG data analysis showed that the EMG activity in the time window between 100 and 0 ms before load onset was higher in the regular condition for the APB [$t(13) = -2.579$, $P = 0.023$] and the FDI [$t(13) = -2.948$, $P = 0.011$] muscles. Across conditions, this activity was positively correlated with the LLR magnitude recorded from the APB and the FDI muscles (Pearson's correlation test, $r = 0.903$, $P < 0.001$ and $r = 0.657$, $P < 0.001$, respectively).

ERP analysis

Waveforms of the grand average data, recorded over the mid sensorimotor area are shown in Fig. 2 (*2nd plot* from the *top*). The waveform represents the mean of electrodes Cz, CCP1h, CCP2h and CPz, the selection of which was based on the scalp distribution of the preparatory activity (see Fig. 5). Preparatory cortical activity is represented in a slow brain potential of negative polarity, which starts at ~1,000 ms before load onset and shows a clear differentiation between the two conditions from ~750 ms before load onset. The mean amplitude from 500 to 0 ms before the load onset, measured in the midline area of interest, was -2.0 ± 0.4 and -0.7 ± 0.2 (SE) μV for the regular and the random condition, respectively. Twelve of 14 participants showed higher (i.e., more negative) preparatory activity in the regular condition. *Participant 14* showed no modulation, and *participant 9* showed higher preparatory activity in the random condition. Despite these two participants, a paired *t*-test demonstrated a significant difference [$t(13) = 4.445$, $P = 0.001$] between the two conditions.

The scalp distribution of the preparatory activity was also represented as a current source density (CSD) map to enhance spatial detail (cf. Perrin et al. 1989), generated for the time interval between 200 and 0 ms before load onset. The CSD distribution suggests that the late preparatory activity might originate from the convexity, i.e., the left and right sensorimotor areas. The statistical *t*-map for this time interval showed a greater difference over the contralateral sensorimotor cortex than over the ipsilateral sensorimotor cortex (see Fig. 5).

Analysis of the postload EEG waveforms revealed a component of similar orientation and location as a P54-N54 component studied by MacKinnon et al. (2000) that they identified as the source of the descending corticospinal output of the LLR. In the present data, this component peaked at 58 ms after load onset and was thus termed N58-P58 component. The topographical maps (Fig. 6) of the grand average data show that this component was generated by a tangential dipolar source with the negative pole over the mid frontal areas and the

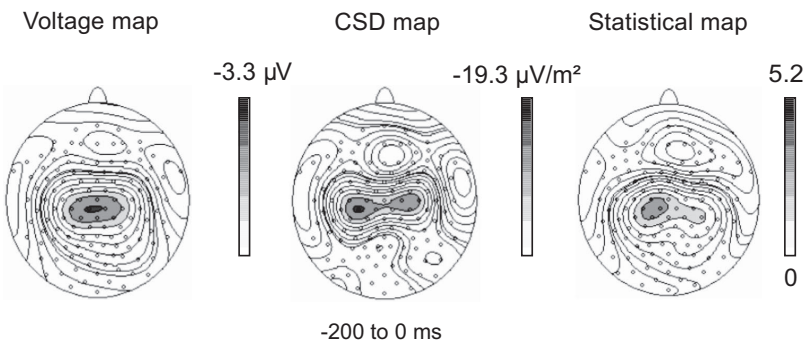

FIG. 5. Scalp voltage distribution (*left*) and current source density distribution (*middle*) of the preparatory activity in the regular condition in the time window between 200 and 0 ms before load onset. Statistical parametric map (*t*-map) of the difference (*right*) between regular and random condition in the same time window (critical *t*-value for $P < 0.05$: 2.16).

TABLE 1. *Peak amplitude of the long-latency reflex (LLR) for random and regular conditions recorded from the APB and FDT muscles*

	Abductor Pollicis Brevis		First Dorsal Interosseous	
	LLR peak amplitude, μV		LLR peak amplitude, μV	
Participant	Random condition	Regular condition	Random condition	Regular condition
1	49.1	29.4	5.4	3.5
2	4.1	3.8	5.7	4.2
3	6.6	12.7	16.7	20.5
4	10.1	2.5	12.4	5.8
5	18.0	12.8	9.0	7.5
*6**	3.5	3.9	3.0	2.6
7	42.8	33.7	3.0	2.4
8	13.8	10.8	14.6	11.8
9	45.8	30.9	41.8	65.4
10	5.2	5.0	5.8	7.0
11	2.2	0.7	4.1	2.9
12	2.8	0.9	3.8	2.9
*13**	3.5	2.0	3.3	2.3
14	17.6	19.4	10.0	8.7
Mean SE	16.0 ± 4.5	12.0 ± 3.2	9.9 ± 2.7	10.5 ± 4.4

Values are means ± SE. *, left-handed participants.

positive pole over the left parietal cortex. The amplitude of the N58-P58, measured as the sum of the negative peak maximum at F1 and the positive peak maximum at CP3, was significantly smaller in the regular compared with the random condition [$t(13) = 5.826$, $P < 0.001$]. To quantify the strength of motor cortex activation and to determine the location and orientation of its source we also performed a dipole source analysis, presented in the next section. Table 1.

Dipole source analysis

The N58-P58 component was modeled in the individual participant data using a single dipole source, separately for the random and the regular conditions. The dipole source models explained the recorded data with a residual variance always <26%. The mean ± SE residual variance was 12.2 ± 2.2% for the regular condition and 8.3 ± 1.4% for the random condition. For all the participants, the location and the orientation of the dipole were virtually identical for the random and regular conditions (Fig. 7).

The tangential orientation and frontal negative maximum of the source were compatible with a motor cortex generator in the anterior wall of the central sulcus. The azimuth and the polar angle defining the source orientation were (mean ± SE) $\theta = 92 \pm 4°$ and $\varphi = 248 \pm 4°$ for the random condition and $\theta = 91 \pm 4°$ and $\varphi = 246 \pm 4°$ for the regular condition. The Talairach-Tournoux coordinates correspond to a precentral generator location, both for the random ($x = -38 \pm 1$, $y = -15 \pm 2$, $z = 44 \pm 2$) and for the regular condition ($x = -39 \pm 2$, $y = -16 \pm 3$, $z = 46 \pm 3$).

The onset and peak latencies of the source waveforms as well as the dipole source strength are presented in Table 2. There was no statistical difference between the two conditions in onset latency [$t(13) = -1.062$, $P = 0.308$] nor in peak latency, although the latter approached significance [$t(13) = -2.007$, $P = 0.066$]. The source strength was higher in the random condition [$t(13) = 2.499$, $P = 0.027$]. Note that this result corresponds with the analysis based on scalp amplitude values taken at F1 and CP3 except for a lower significance level in the dipole source analysis. Also noteworthy, in both analysis approaches *participants 9* and *14,* who showed a reversed and absent preparatory EEG modulation, respectively, were found to have a reversed N58-P58 modulation.

DISCUSSION

The purpose of this study was to determine the functional role of cortical activity associated with stabilization of an object held in precision grip. The results show that preparatory slow brain potentials accompany preparatory adjustments in grip force preceding temporally predictable load force pertur-

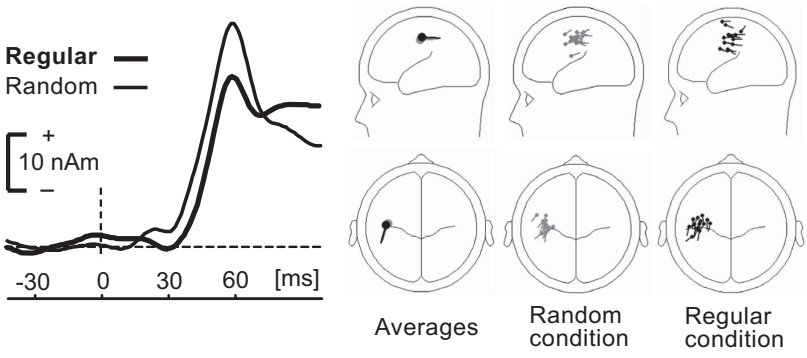

FIG. 7. Dipole source waveforms averaged across subjects ($n = 14$), mean N58-P58 dipole source location and orientation, and individual dipole sources.

TABLE 2. *N58-D58 parameters in dipole source wave forms*

	Random Condition				Regular Condition			
Participant	Onset Latency, ms	Peak Latency, ms	Peak Amplitude, nAm	Residual Variance, %	Onset Latency, ms	Peak Latency, ms	Peak Amplitude, nAm	Residual Variance, %
1	40.1	61.6	59.5	7.6	38.1	60.6	45.6	12.4
2	33.2	58.6	26.4	12.2	31.3	59.6	19.9	24.9
3	33.2	59.6	53.5	2.4	31.3	63.5	32.6	7.6
4	33.2	60.6	27.7	7.6	31.3	58.6	17.8	6.1
5	31.3	57.6	60.9	6.1	32.2	59.6	56.8	3.0
*6**	31.3	57.6	62.2	5.5	30.3	58.6	50.3	4.3
7	26.4	46.9	32.0	6.9	29.3	49.8	13.4	25.6
8	34.2	59.6	43.5	15.0	33.2	58.6	39.3	14.3
9	45.9	56.7	47.7	13.0	44.9	56.7	69.2	6.9
10	32.2	60.6	59.4	3.5	38.1	60.6	44.4	6.5
11	35.2	61.6	64.9	3.0	36.2	61.6	54.5	3.3
12	33.2	60.6	20.6	5.8	39.1	63.5	6.3	17.0
*13**	29.3	56.7	32.0	7.1	36.2	58.6	16.1	23.6
14	35.2	49.8	25.7	25.7	35.2	50.8	39.0	15.0
Mean	33.8	57.7	44.0	8.2	34.8	58.6	36.1	12.2
SE	1.2	1.2	4.3	1.4	1.2	1.1	5.1	2.2

*: Left-handed participants.

bations. Predictability of load force perturbations also influenced sensorimotor cortex activity immediately preceding the long-latency reflex. The preparatory activity may be seen as modulating the long-latency reflex, mediated by the sensorimotor cortex activity preceding the reflex. In the following, we first discuss the preparatory activity, then the modulation of the long-latency reflex.

Anticipatory activity preceding load force perturbations

The experimental manipulation of predictably timed versus randomly timed load force perturbations has a background in earlier work on precision grip (Boudreau and Smith 2001; Kwok and Wing 2006; Weeks et al. 2000) but also in a body of work concerning the influence of temporal (un)certainty on response times (Niemi and Näätänen 1981). Predictably timed reaction signals provide the opportunity to prepare for a specific response in the case of simple reaction tasks but also confer an advantage in choice tasks, where temporal preparation optimizes "response readiness." Neurophysiological signs of adjustment to the temporal structure of a task have been reported in the form of slow preparatory brain potentials, in particular the contingent negative variation or CNV (Walter et al. 1964). The time course and amplitude of slow brain potentials are influenced by the temporal structure of a task not only when participants are made aware of a timing manipulation (Müller-Gethmann et al. 2003) or have an explicit timing instruction (Walter et al. 1964) but also when timing is manipulated in an implicit fashion (Praamstra et al. 2006).

The preparatory slow brain potential recorded in the present study is related to the CNV (Walter et al. 1964). The higher amplitude in the predictable condition is consistent with earlier work comparing the CNV during fixed and variable intertrial intervals (Cunnington et al. 1995). As to the neural substrate underlying the preparatory negative slow waves, in a neuroimaging investigation the preparation for a predictable simple movement was found to depend on primary sensorimotor cortex and medial premotor cortex (Jenkins et al. 2000). Preparation for a temporally predictable choice response also involves lateral (pre)motor structures, as we demonstrated in an earlier EEG study (Praamstra et al. 2006). In the present data, the preparatory activity showed a scalp distribution with midline fronto-central maximum, only to develop a contralateral predominance in the last 200 ms before load onset. The distribution is compatible with contributions from medial but also from lateral premotor and/or sensorimotor cortex. Note that the distribution of the lateralized activity maintained a monopolar form rather than developing into a dipolar distribution. Hence this preparatory activity has not the same origin as the sensorimotor cortex activation represented by the N58-P58. Even so, it must be assumed that this activity was responsible for the preparatory increase of EMG and force preceding predictable load force perturbations, while at the same time reflecting temporal preparation that presets relevant brain structures for the anticipated load force perturbation and thus influencing the N58-P58.

The robust preparatory activity evidenced here in slow brain potentials contrasts with remarkably little preparatory activity in single-unit responses from cells in primary motor cortex (Picard and Smith 1992), dorsal and ventral premotor cortex (Boudreau et al. 2001), and the medial wall premotor areas (supplementary and cingulate motor areas) (Cadoret and Smith 1997). In these studies, preparatory single-unit activity was virtually absent notwithstanding the presence of preparatory grip force adjustments, suggesting that these motor areas are not significantly involved in the elaboration of adaptive internal models of hand-object dynamics (Boudreau et al. 2001). The discrepancy might be due to the slow brain potentials reflecting a general adaptation to the temporally predictable timing regime without actual connection to the mechanisms controlling reflex grip force adjustments. However, although this explanation cannot be entirely ruled out, our data point to an association between the presence of preparatory activity and the amplitude of motor cortical potentials preceding the reflex. Also relevant to the discrepancy is the fact that the preparatory EEG activity reflects postsynaptic dendritic potentials different from single-unit action potentials. The slow brain potentials may modulate cortical excitability and reflex amplitude with-

out direct reflection in cell action potentials. Nevertheless, this still leaves unexplained why there is preparatory grip force adjustment without concomitant spiking activity.

Motor cortex potentials after load force perturbations

Goodin et al. (1990) described a direct relationship between the amplitude of scalp-recorded vertex maximal EEG potentials and the LLR amplitude. The amplitudes of these cerebral and EMG responses were attenuated after predictable perturbations. MacKinnon et al. (2000) identified motor cortical potentials preceding the long-latency stretch reflex, peaking at a latency of 54 ms after forced wrist extension. The authors interpreted these potentials as reflecting synaptic input onto corticospinal neurons. In the present data, we found similar motor cortical potentials peaking at 58 ms after the load perturbation. In contrast to the MacKinnon et al. (2000) study, the motor cortical potentials were modulated by the task. In addition, we identified preparatory cortical activity preceding the load force perturbation that might underlie the modulation of the sensorimotor cortex activity expressed in the N58-P58. The timing of the N58-P58 was consistent with the onset and peak latency of the EMG LLR. This suggests that the long-latency reflex is not only transcortical but also that it is modulated at a central level. This suggestion contrasts with MacKinnon et al. (2000), who localized the modulation of the LLR by task conditions downstream from the primary motor cortex.

An unfortunate weakness of the present study was that preparatory EMG activity was found for the FDI muscle but that the LLR modulation of the FDI was not as clear as for the APB. The width of the manipulandum (7.4 cm) was very close to many participants' maximal grip aperture, and we suspect that this may have attenuated the reflex response in the FDI and thus obscured its modulation. A related issue is the possible confounding effect of preparatory EMG amplitude on the LLR. It has been shown that the LLR magnitude increases with increased preload muscle activity (Marsden et al. 1976). Capaday et al. (1994) demonstrated a nearly linear relationship between background EMG activity and LLR amplitude. In our data, across participants and conditions, the LLR amplitude was also positively correlated with preload EMG activity. Nonetheless, increased (preparatory) EMG activity in the regular condition was accompanied by a decrease in LLR magnitude relative to the random condition. The positive correlation between preload EMG and LLR magnitude, however, may have attenuated this modulation. Relevant in this context is that the grip force response was modulated in the expected direction with a smaller response after regular than after randomly timed perturbations. Although the direction of the modulation can be taken as reliable, the modulation showed a lag relative to the LLR and may have been affected by the cross-talk problem causing a grip force response coincident with the load perturbation.

It has to be acknowledged that the N58-P58 was not modulated in isolation. Evoked responses after the N58-P58 (P100, N140) also differed between regular and randomly timed load force perturbations. A reduction in amplitude of median nerve somatosensory evoked potentials is observed when they are elicited during tactile exploration, movement, or imagined movement (Cheron and Borenstein 1992; Huttunen and Hömberg 1991; Jones et al. 1989). A similar movement-related "gating" of evoked responses may have been invoked in the regular condition of our experiment, thus accounting for at least part of the amplitude differences observed. Whether or not the modulation of the N58-P58 involves more than just this mechanism cannot be answered with certainty. Although our data suggest a relation of the N58-P58 with the efferent limb of the LLR reflex arc, this needs to be further substantiated by data that show a convincing co-variation of the amplitude of the N58-P58 and the magnitude of the LLR.

The identification of sensorimotor cortex potentials preceding reflex grip adjustments might raise the question whether the reflex was cutaneously mediated or due to muscle stretch. This is because the muscle-stretch-mediated long-latency reflex seems better accepted as transcortical than the cutaneously-mediated long-latency reflex (Macefield et al. 1996b). However, the available evidence is mixed. From microneurographic data, Macefield et al. (1996a) inferred that tactile afferents rather than muscle afferents mediate reflex grip adjustments following load perturbations. Corden et al. (2000) also provided evidence that the origins of the long-latency reflex recorded from the FDI muscle are the skin and/or subcutaneous nerve terminals. At the motor cortex level, cells receiving cutaneous afferents and cells receiving proprioceptive afferents both fire at latencies short enough to contribute to the long-latency reflex (Boudreau and Smith 2001; Picard and Smith 1992). Yet the excitation of motor cortex neurons through cutaneous afferents was reported as stronger than that through proprioceptive feedback (Picard and Smith 1992). Taken together, the possibility of a transcortical route for tactile information triggering the long latency reflex is certainly not contradicted by existing evidence.

Conclusion

This study identified movement-related EEG correlates of grip force adjustments preceding predictable load perturbations. Movement-related activity in motor areas of the cortex is expected to accompany anticipatory grip force increase but has not been detected in studies using single-cell recordings in monkeys. The preparatory EEG activity identified in the present study probably also presets relevant structures for the anticipated load force perturbation, thus reducing the long-latency reflex response to predictable compared with randomly timed perturbations. Our data suggest that the locus of this modulation is central reflected in an AM of the phasic sensorimotor cortex activity immediately preceding the long latency reflex. In a previous study that also used EEG, MacKinnon et al. (2000) did not find a similar central modulation for the muscle stretch-mediated long-latency reflex, although their results supported a transcortical pathway. This difference may reflect a difference between proprioceptive and tactile mediation of the long-latency reflex but is perhaps more likely explained by the different ways in which the experiments manipulated preparatory set. Further work is needed, however, to clarify this difference and establish an unambiguous co-variation between sensorimotor cortex activity and reflex amplitude to underpin a central modulation of the long-latency reflex.

ACKNOWLEDGMENTS

A. Witney contributed to the software controlling the Phantom robot. We are grateful to two anonymous reviewers for their constructive comments.

GRANTS

This work was supported by the Medical Research Council, UK under Grant MRC G9901257.

REFERENCES

American Electroencephalographic Society. Guideline thirteen: guidelines for standard electrode position nomenclature. American Electroencephalographic Society. *J Clin Neurophysiol* 11: 111–113, 1994.

Boudreau M, Brochier T, Pare M, Smith AM. Activity in ventral and dorsal premotor cortex in response to predictable force-pulse perturbations in a precision grip task. *J Neurophysiol* 86: 1067–1078, 2001.

Boudreau M, Smith AM. Activity in rostral motor cortex in response to predictable force-pulse perturbations in a precision grip task. *J Neurophysiol* 86: 1079–1085, 2001.

Cadoret G, Smith AM. Comparison of the neuronal activity in the SMA and the ventral cingulated cortex during prehension in the monkey. *J Neurophysiol* 77: 153–166, 1997.

Cheron G, Borenstein S. Mental movement simulation affects the N30 frontal component of the somatosensory evoked potential. *Electroencephalogr Clin Neurophysiol* 84: 288–92, 1992.

Capaday C, Forget R, Milner T. A re-examination of the effects of instruction on the long-latency stretch reflex response of the flexor pollicis longus muscle. *Exp Brain Res* 100: 515–521, 1994.

Corden DM, Lippold OCJ, Buchanan K, Norrington C. Long-latency component of the stretch reflex in human muscle is not mediated by intramuscular skin receptors. *J Neurophysiol* 84: 184–188, 2000.

Cunnington R, Iansek R, Bradshaw JL, Phillips JG. Movement-related potentials in Parkinson's disease. Presence and predictability of temporal and spatial cues. *Brain* 118: 935–50, 1995.

Dugas C, Smith AM. Responses of cerebellar purkinje cells to slip of a hand-held object. *J Neurophysiol* 68: 483–495, 1992.

Ehrsson H, Fagergren A, Johansson RS, Forssberg H. Evidence for the involvement of the posterior parietal cortex in coordination of fingertip forces for grasp stability in manipulation. *J Neurophysiol* 90: 2978–2986, 2003.

Flanagan JR, Vetter P, Johansson RS, Wolpert DM. Prediction precedes control in motor learning. *Curr Biol* 13: 146–50, 2003.

Flanagan JR, Wing AM. Modulation of grip force with load force during point-to-point arm movements. *Exp Brain Res* 95: 131–143, 1993.

Flanagan JR, Wing AM. The role of internal models in motion planning and control: evidence from grip force adjustments during movements of hand-held loads. *J Neurosci* 17: 1519–1528, 1997.

Goodin DS, Aminoff MC, Shih PY. Evidence that the long-latency reflex responses of the human wrist extensor muscle involve a transcerebral pathway. *Brain* 113: 1075–1091, 1990.

Huttunen J, Hömberg V. Modification of cortical somatosensory evoked potentials during tactile exploration and simple active and passive movements. *Electroencephalogr Clin Neurophysiol* 81: 216–23, 1991.

Jenkins IH, Jahanshahi M, Jueptner M, Passingham RE, Brooks DJ. Self-initiated versus externally triggered movements. II. The effect of movement predictability on regional cerebral blood flow. *Brain* 123: 1216–1228, 2000.

Johansson RS, Lemon RN, Westling G. Time-varying enhancement of human cortical excitability mediated by cutaneous inputs during precision grip. *J Physiol* 481: 761–775, 1994.

Johansson RS, Westling G. Roles of glabrous skin receptors and sensorimotor memory in automatic control of precision grip when lifting rougher or more slippery objects. *Exp Brain Res* 56: 550–564, 1984.

Jones SJ, Halonen JP, Shawkat F. Centrifugal and centripetal mechanisms involved in the "gating" of cortical SEPs during movement. *Electroencephalogr Clin Neurophysiol* 74: 36–45, 1989.

Kawato M, Kuroda T, Imamizu H, Nakano E, Miyauchi S, Yoshioka T. Internal forward models in the cerebellum: fMRI study on grip force and load force coupling. *Prog Brain Res* 142: 171–188, 2003.

Kinoshita H, Oku N, Hashikawa K, Nishimura T. Functional brain areas used for the lifting of objects using a precision grip: a PET study. *Brain Res* 857: 119–130, 2000.

Kwok HF, Wing AM. Time-based prediction in motor control: evidence from grip force response to external load perturbations. *Exp Brain Res* 175: 183–190, 2006.

Lee RG, Tatton WG. Motor responses to sudden limb displacements in primates with specific CNS lesions and in humans patients with motor system disorders. *Can J Neurol Sci* 2: 285–293, 1975.

Macefield VG, Hager-Ross C, Johansson RS. Control of grip force during restraint of an object held between finger and thumb: responses of cutaneous afferents from the digits. *Exp Brain Res* 108: 155–171, 1996a.

Macefield VG, Rothwell JC, Day BL. The contribution of transcortical pathways to long-latency stretch and tactile reflexes in human hand muscles. *Exp Brain Res* 108: 147–154, 1996b.

MacKinnon CD, Verrier MC, Tatton WG. Motor cortical potentials precede long-latency EMG activity evoked by imposed displacements of the human wrist. *Exp Brain Res* 131: 477–490, 2000.

Marsden CD, Merton PA, Morton HB. Servo action in the human thumb. *J Physiol* 257: 1–44, 1976.

Milner TE, Franklin DW, Imamizu H, Kawato M. Central representation of dynamics when manipulating handheld objects. *J Neurophysiol* 95: 893–901, 2006.

Monzee J, Smith AM. Responses of cerebellar interpositus neurons to predictable perturbations applied to an object held in a precision grip. *J Neurophysiol* 91: 1230–1239, 2004.

Müller-Gethmann H, Ulrich R, Rinkenauer G. Locus of the effect of temporal preparation: evidence from the lateralized readiness potential. *Psychophysiol* 40: 597–611, 2003.

Napier JR. The prehensile movements of the human hand. *J Bone Joint Surg* 38B: 902–913, 1956.

Niemi P, Näätänen R. Foreperiod and simple reaction time. *Psychol Bull* 89: 133–162, 1981.

Oostenveld R, Praamstra P. The five percent electrode system for high-resolution EEG and ERP measurements. *Clin Neurophysiol* 112: 713–719, 2001.

Perrin F, Pernier J, Bertrand O, Echallier JF. Spherical splines for scalp potential and current density mapping. *Electroencephalogr Clin Neurophysiol* 72: 184–187, 1989.

Picard N, Smith AM. Primary motor cortical responses to perturbations of prehension in the monkey. *J Neurophysiol* 68: 1882–1894, 1992.

Praamstra P, Kourtis D, Kwok HF, Oostenveld R. Neurophysiology of implicit timing in serial choice reaction-time performance. *J Neurosci* 26: 5448–5455, 2006.

Schmitz C, Jenmalm P, Ehrsson HH, Forssberg H. Brain activity during predictable and unpredictable weight changes when lifting objects. *J Neurophysiol* 93: 1498–1509, 2005.

Serrien DJ, Kaluzny P, Wicki U, Wiesendanger M. Grip force adjustments induced by predictable load perturbations during a manipulative task. *Exp Brain Res* 124: 100–106, 1999.

Turrell YN, Li FX, Wing AM. Grip force dynamics in the approach to a collision. *Exp Brain Res* 128: 86–91, 1999.

Walter WG, Cooper R, Aldridge VJ, McCallum WC, Winter AL. Contingent negative variation: an electric sign of sensorimotor association and expectation in the human brain. *Nature* 203: 380–384, 1964.

Weeks DL, Wallace SA, Noteboom JT. Precision-grip force changes in the anatomical and prosthetic limb during predictable load increases. *Exp Brain Res* 132: 404–410, 2000.

Wing AM, Flanagan JR. Forward models for motion planning. *Pro ASME Dynam Syst Control Div* 64: 139–143, 1998.